



# A sensitive mass spectrum assay to characterize engineered methionine adenosyltransferases with *S*-alkyl methionine analogues as substrates



Rui Wang<sup>a,b</sup>, Weihong Zheng<sup>a</sup>, Minkui Luo<sup>a,\*</sup>

<sup>a</sup> Molecular Pharmacology and Chemistry Program, Memorial Sloan–Kettering Cancer Center, New York, NY 10065, USA

<sup>b</sup> Program of Pharmacology, Weill Graduate School of Medical Science, Cornell University, New York, NY 10021, USA

## ARTICLE INFO

### Article history:

Received 20 August 2013

Received in revised form 16 December 2013

Accepted 18 December 2013

Available online 27 December 2013

### Keywords:

Epigenetics

Methyltransferase

MAT

*S*-Adenosyl-*L*-methionine

LC–MS/MS

## ABSTRACT

Methionine adenosyltransferases (MATs) catalyze the formation of *S*-adenosyl-*L*-methionine (SAM) inside living cells. Recently, *S*-alkyl analogues of SAM have been documented as cofactor surrogates to label novel targets of methyltransferases. However, these chemically synthesized SAM analogues are not suitable for cell-based studies because of their poor membrane permeability. This issue was recently addressed under a cellular setting through a chemoenzymatic strategy to process membrane-permeable *S*-alkyl analogues of methionine (SAAMs) into the SAM analogues with engineered MATs. Here we describe a general sensitive activity assay for engineered MATs by converting the reaction products into *S*-alkylthioadenosines, followed by high-performance liquid chromatography–tandem mass spectrometry (HPLC–MS/MS) quantification. With this assay, 40 human MAT mutants were evaluated against 7 SAAMs as potential substrates. The structure–activity relationship revealed that, besides better engaged SAAM binding by the MAT mutants (lower  $K_m$  value in contrast to native MATs), the gained activity toward the bulky SAAMs stems from their ability to maintain the desired linear  $S_N2$  transition state (reflected by higher  $k_{cat}$  value). Here the I117A mutant of human MAT1 was identified as the most active variant for biochemical production of SAM analogues from diverse SAAMs.

© 2013 Elsevier Inc. All rights reserved.

*S*-Adenosyl-*L*-methionine (SAM),<sup>1</sup> one of the most commonly used enzyme cofactors, is found among all living organisms [1,2]. The biochemical reactivity of SAM is largely embedded within its three carbon sulfonium bonds as well as their neighboring regions [2–4]. For instance, the two alkyl sulfonium bonds can undergo enzyme-mediated homolytic cleavage to yield the canonical 5'-deoxyadenosyl or noncanonical 3-amino-3-carboxypropyl radical [5,6]. In contrast, the methyl sulfonium bond is often subjected to the heterolytic cleavage to render a methyl electrophile for diverse acceptors ranging from large DNA, RNA, and protein complexes to small-molecule metabolites [7]. In conjunction with the increased interest in these transformations, multiple SAM analogues have been documented to probe reactions or mechanisms of SAM-using enzymes, including methyltransferases [8–10]. Among the early examples was to replace SAM's sulfonium moiety with selenium to examine

the effect of the weaker carbon chalcogen bond on catalytic turnover [11]. As recently demonstrated by our laboratory and others, bulky sulfonium- $\beta$ -sp<sup>2</sup>/sp<sup>1</sup>-alkyl analogues of SAM can serve as cofactor surrogates of native or engineered methyltransferases for substrate labeling or profiling [9,12–23].

To access bulky sulfonium-alkyl analogues of SAM, most previous efforts relied on chemical alkylation of *S*-adenosyl-*L*-homocysteine (SAH) with the corresponding alkyl electrophiles [12–23]. However, besides the limitation of less desirable yields and requiring laborious high-performance liquid chromatography (HPLC) purification [12–23], chemically synthesized SAM analogues often consist of diastereomeric mixtures with only the sulfonium-(*S*)-epimer bioactive [12–24]. More important, SAM analogues generally show poor membrane permeability, which limits their use in a cellular setting [8].

Within living cells, SAM is mainly generated by methionine adenosyltransferases (MATs) with endogenous methionine and ATP as substrates and phosphate and pyrophosphate as byproducts (Fig. 1) [2,16]. An alternative biosynthesis of SAM involves the SAH-catalyzed reverse transformation with methionine and 5'-chloro-5'-deoxyadenosine as substrates [22]. The general *in vivo* setting of MATs also inspired us to develop a chemoenzymatic strategy with engineered MATs to process membrane-permeable *S*-alkyl analogues of methionine (SAAMs or *S*-alkyl-*L*-homocysteines) into

\* Corresponding author.

E-mail address: [luom@mskcc.org](mailto:luom@mskcc.org) (M. Luo).

<sup>1</sup> Abbreviations used: SAM, *S*-adenosyl-*L*-methionine; SAH, *S*-adenosyl-*L*-homocysteine; HPLC, high-performance liquid chromatography; MAT, methionine adenosyltransferase; SAAM, *S*-alkyl analogue of methionine (*S*-alkyl-*L*-homocysteine); NADPH, nicotinamide adenine dinucleotide phosphate; NMR, nuclear magnetic resonance; DMSO, dimethyl sulfoxide; UV, ultraviolet; LC–MS, liquid chromatography–mass spectrometry; ESI, electron spray ionization; MRM, multiple reaction monitoring; MS/MS, tandem mass spectrometry; MTA, 5'-methylthioadenosine.

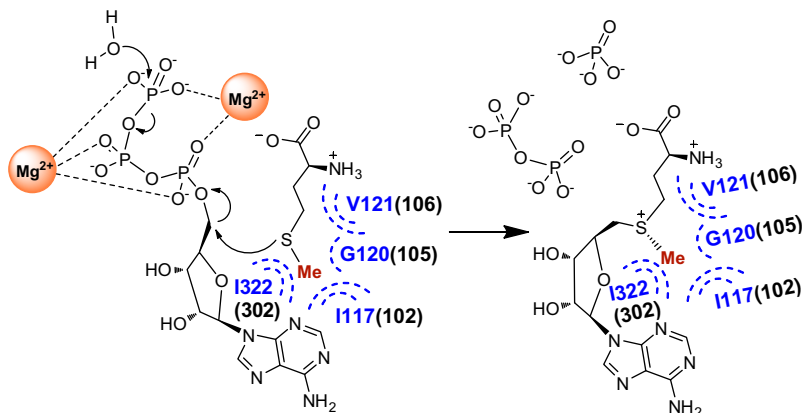


**Fig. 1.** MAT-catalyzed SAM production with methionine and ATP as substrates and phosphate and pyrophosphate as byproducts. Here the residues adjacent to S-methyl moiety of the substrate methionine are constructed and highlighted on comparing human MATI and MATII (blue, PDB 2OBV and 2P02) and *Escherichia coli* MAT (black in parentheses) as reported previously [29].

the SAM analogues [16]. Despite the previous proof-of-concept use of the engineered MAT in vitro and inside living cells [16], few efforts have been made to systematically characterize these MAT variants, likely because of the lack of a general activity assay for MAT mutants with diverse SAAMs as substrates and SAM analogues as products [16,25–27]. Given the potential use of the chemoenzymatic strategy for multiple SAM-using enzymes, as exemplified recently by methyltransferases [12–23], here we document a sensitive, generally applicable mass-spectroscopy-based assay to quantify SAM analogues (Fig. 2).

The conventional kinetic analysis of MATs was carried out through HPLC-based spectroscopic quantification of the reaction product SAM, a less sensitive assay format that often requires a large amount of reaction materials [25]. Alternatively, less environmentally friendly radiolabeled methionine or ATP can be used as a substrate with the reaction product SAM isolated by chromatography and quantified by a scintillation counter [26]. Recently, a more sensitive spectroscopic MAT assay was developed by monitoring the production of nicotinamide adenine dinucleotide phosphate (NADPH) from the reaction byproduct pyrophosphate using three coupling enzymes: uridine diphosphoglucose pyrophosphorylase,

phosphoglucosyltransferase, and glucose 6-phosphate dehydrogenase [27]. This continuous assay is sensitive but can be affected by potential cellular components interfering with the coupling enzymes or NADPH readout. Here we describe a sensitive mass-spectroscopy-based assay by converting SAM and S-alkyl analogues of SAM (the reaction products of native and engineered MATs) into S-alkyl thioadenosines for quantification (Fig. 2). This assay is further featured by its potential application to quantify S-alkyl analogues of SAM in complex cellular settings. We implemented the assay to evaluate activities of 40 MAT variants toward 7 SAAMs as potential substrates. The structure–activity relationship revealed that the difference of the overall catalytic efficiency ( $k_{\text{cat}}/K_m$  values) of engineered MATs toward bulky SAAMs largely arises from the values of  $k_{\text{cat}}$  reflected at the chemical step and enzymatic transition state, whereas the values of  $K_m$  for binding substrates are comparable among diverse SAAMs. This observation argues for the importance of engineering MATs to both bind bulky substrates (the step reflected by small  $K_m$  values) and efficiently process them into products through active enzymatic transition states (the step reflected by decent  $k_{\text{cat}}$  values). Here the I117A mutant of human MATI was identified to be the most active MAT

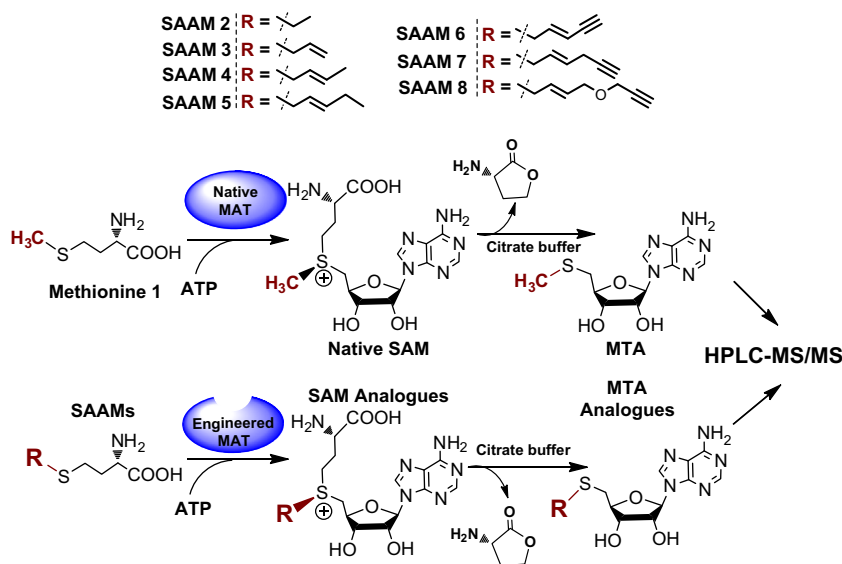


**Fig. 2.** Schematic presentation of MS-based MAT activity assay. In this assay, SAM/SAM analogues were quantitatively converted into the corresponding MTA/MTA analogues and lactone through intramolecular lactonization, followed by tandem HPLC–MS/MS quantification.

variant for biochemical production of sulfonium-alkyl analogues of SAM from diverse SAAMs.

## Materials and methods

### General materials and methods

SAM, SAH, L-methionine **1**, S-ethyl analogue of methionine (L-ethionine, **2**), and the reagents for chemical synthesis were obtained from Aldrich Chemical and used without further purification. Optima-grade acetonitrile was obtained from Fisher Scientific and degassed under vacuum prior to HPLC purification. Citrate buffer was purchased from Sigma–Aldrich (cat. no. 83273). Cocktail of ethylenediaminetetraacetic acid (EDTA)-free protease inhibitors was purchased from Roche Applied Science. Aqueous solutions of SAAMs were concentrated with a Savant Sc210A SpeedVac concentrator (Thermo) and then lyophilized with a Flexi-Dry  $\mu$ P Freeze-Dryer (FTS system). Nuclear magnetic resonance (NMR) spectra were recorded on a Burke AVIII 500- or 600-MHz spectrometer. NMR chemical shifts are reported in ppm; multiplicity is indicated by s (singlet), d (doublet), t (triplet), q (quartet), m (multiplet), dd (doublet of doublet), and so forth; coupling constants ( $J$ ) are reported in Hz with peak integration provided. Occasionally, formic acid- $d_2$  of 5  $\mu$ l was added into 600  $\mu$ l of  $D_2O$  as the NMR solvent to increase the solubility of the compounds containing an  $\alpha$ -amino acid moiety.  $^1H/^{13}C$  NMR chemical shifts were referenced to solvent peaks (residual  $^1H$  in  $D_2O$  and dimethyl sulfoxide [DMSO]- $d_6$  = 4.79 ppm and 3.50 ppm, respectively; residual  $^{13}C$  in formic acid- $d_2$  and DMSO- $d_6$  = 166.2 ppm and 39.7 ppm, respectively). Analytical HPLC was carried out on a Waters 600 controller HPLC/2998 diode array detector using an XBridge Prep C18 reverse phase column (5  $\mu$ m,  $4.6 \times 150$  mm). Preparative HPLC purification was carried out on a DELTA PAK C18 column (15  $\mu$ m, 300 A,  $300 \times 3.9$  mm) or an XBridge Prep C18 reverse phase column (5  $\mu$ m, OBD,  $19 \times 150$  mm) with ultraviolet (UV) detection at 260 nm. Mass spectral analysis was carried out at the MSKCC Analytical Core Facility on a PE SCIEX API 100 or Waters Acuity SQD liquid chromatography–mass spectrometry (LC–MS) system with electron spray ionization (ESI). LC–MS samples were analyzed by multiple reaction monitoring (MRM) modes using the 6410 tandem LC–MS/MS system (Agilent Technologies) coupled with a Zorbax Eclipse XDB-C18 column ( $2.1 \times 50$  mm, 3.5  $\mu$ m).

### Synthesis, purification, and characterization of SAAMs **2** to **8**

S-Ethyl analogue of methionine (SAAM **2**, L-ethionine) is available from Sigma–Aldrich. S-Benzyl-L-homocysteine and S-allyl-L-homocysteine (SAAM **3**) were prepared as reported previously [28]. To prepare SAAMs **4** to **8** (Scheme 1), S-benzyl-L-homocysteine (255 mg, 1 mmol) [29] was placed in a round-bottom flask connected to an ammonia cylinder and dissolved in approximately 20 ml of condensed liquid ammonia in a dry ice–ethanol bath. Sodium metal (50 mg, 2.2 mmol) was then added gradually to afford a dark blue solution. After the dark blue solution became colorless a few minutes later, the dry ice–ethanol bath was removed to allow the evaporation of ammonia. The remaining trace of ammonia was removed with the aid of a flow of argon, followed by vacuum for 3 h.

The resultant white solid was dissolved in dry ethanol (10 ml) and cooled down to 0 °C. A solution of tosylate or bromide (1.05 mmol) in ethanol (3 ml) was added (bromides for the synthesis of SAAMs **3**, **4**, **7**, and **8**; tosylates for SAAMs **5** and **6**) [16–19,21,22]. This reaction mixture was stirred at 0 °C for 1 h and then brought to ambient temperature (23 °C) overnight. Solvent was then removed by rotary evaporation, and the resultant residue was redissolved in water (5 ml) and purified using a self-packed  $1.5 \times 5$ -cm Dowex 50 ( $H^+$ ) cation exchange column. The column was washed with water until the pH of the eluent became neutral. The products were then eluted from the column using 5% ammonia hydroxide, which was later removed by rotary evaporation. The portions containing the expected products (monitored by silica gel thin layer chromatography [TLC] with the eluting solvent,  $n$ -BuOH/AcOH/ $H_2O$  4:1:1; the staining protocol, 0.2% ninhydrin in 96% EtOH/AcOH/s-collidine 6:3:1 on heating) were combined and concentrated on a rotary evaporator to yield a white solid. The crude products were then dissolved in 0.1 N HCl and subject to further purification with a preparative reverse phase HPLC system (XBridge Prep C18 column, 5- $\mu$ m, OBD,  $19 \times 150$  mm). The final products were eluted by a solvent of a linear gradient from 10 to 60% of acetonitrile in aqueous trifluoroacetic acid (0.1%) for 15 min with a flow rate of 10 ml/min. The desired fractions were combined and lyophilized to yield a white powder (overall yields of 82, 67, 56, 56, 35, and 58% for SAAMs **3**, **4**, **5**, **6**, **7**, and **9**, respectively).

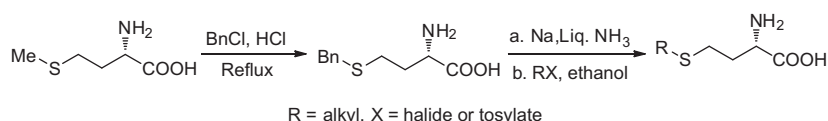
$^1H$  NMR (500 MHz,  $D_2O$ ) of SAAM **3** (S-allyl-L-homocysteine) [28]:  $\delta$  2.07–2.20 (m, 2H), 2.62 (t, 2H,  $J$  = 7.5 Hz), 3.23 (d, 2H,  $J$  = 7.2 Hz), 3.84 (t, 1H,  $J$  = 6.3 Hz), 5.16–5.22 (m, 2H), 5.80–5.88 (m, 1H).

$^1H$  NMR (500 MHz,  $D_2O$ ) of SAAM **4** (S-crotyl-L-homocysteine):  $\delta$  1.71 (d, 3H,  $J$  = 6.4 Hz), 2.15–2.20 (m, 1H), 2.23–2.29 (m, 1H), 2.67 (t, 2H,  $d$  = 7.5 Hz), 3.20 (d, 2H,  $J$  = 7.3 Hz), 4.17 (t, 1H,  $J$  = 6.3 Hz), 5.47–5.53 (m, 1H), 5.70–5.71 (m, 1H);  $^{13}C$  NMR (125 MHz,  $D_2O$ ):  $\delta$  16.88, 24.91, 29.45, 32.50, 52.15, 126.04, 129.92, 172.07; ESI–MS: 190 [M+H] $^+$ . HRMS: calculated for  $C_8H_{16}NO_2S$  ([M+H] $^+$ ) 190.0902, found 190.0897.

$^1H$  NMR (500 MHz,  $D_2O$ ) of SAAM **5** (*trans*-pent-2-enyl-L-homocysteine):  $\delta$  1.02 (t, 3H,  $J$  = 7.4 Hz), 2.09–2.13 (m, 2H), 2.15–2.19 (m, 1H), 2.22–2.23 (m, 1H), 2.68 (t, 2H,  $d$  = 7.3 Hz), 3.23 (d, 2H,  $J$  = 7.2 Hz), 4.01 (t, 1H,  $J$  = 6.2 Hz), 5.50–5.54 (m, 1H), 5.76–5.79 (m, 1H);  $^{13}C$  NMR (150 MHz,  $D_2O$ ):  $\delta$  12.81, 24.70, 24.94, 29.70, 32.41, 53.05, 123.73, 136.90, 173.15; ESI–MS: 204 [M+H] $^+$ . HRMS: calculated for  $C_9H_{18}NO_2S$  ([M+H] $^+$ ) 204.1058, found 204.1056.

$^1H$  NMR (500 MHz,  $D_2O$ +formic acid- $d_2$ ) of SAAM **6** (S-(pent-2-en-4-ynyl)-L-homocysteine):  $\delta$  1.98–2.04 (m, 1H), 2.06–2.12 (m, 1H), 2.50 (t, 2H,  $J$  = 7.4 Hz), 3.12 (d, 2H,  $J$  = 7.4 Hz), 3.15 (s, 1H), 3.99 (t, 1H,  $J$  = 6.0 Hz), 5.50 (d, 1H, 15.7 Hz), 6.06–6.12 (m, 1H);  $^{13}C$  NMR (125 MHz,  $D_2O$  + formic acid- $d_2$ ):  $\delta$  25.99, 30.15, 33.06, 52.86, 79.09, 82.71, 111.45, 142.06, 172.77; MS(ESI)  $m/z$ : 200 [M+H] $^+$ ; HRMS: calculated for  $C_9H_{14}NO_2S$  ([M+H] $^+$ ) 200.0745, found 200.0746.

$^1H$  NMR (500 MHz,  $D_2O$ ) of SAAM **7** (S-(hex-2-en-5-ynyl)-L-homocysteine): 2.13–2.19 (m, 1H), 2.22–2.28 (m, 1H), 2.52 (t, 1H,  $J$  = 2.4 Hz), 2.66 (t, 2H,  $J$  = 7.5 Hz), 3.00–3.02 (m, 2H), 3.23 (dd, 2H,  $J$  = 7.2, 0.7 Hz), 4.14 (t, 1H,  $J$  = 6.3 Hz), 5.64–5.70 (m, 1H), 5.75–5.81 (m, 1H);  $^{13}C$  NMR (150 MHz,  $D_2O$  + formic acid- $d_2$ ):  $\delta$  21.20, 25.68, 30.14, 32.68, 52.78, 71.94, 83.23, 117.00 (q,  $J$  = 289.78), 127.90, 128.37, 163.65 (q,  $J$  = 35.2 Hz), 172.76; MS(ESI)



**Scheme 1.** General synthesis of SAAMs **3** to **8**.

$m/z$ : 214  $[M+H]^+$ ; HRMS: calculated for  $C_{10}H_{16}NO_2S$  ( $[M+H]^+$ ) 214.0902, found 214.0898.

$^1H$  NMR (500 MHz,  $DMSO-d_6$ ) of SAAM **8** (*S*-[4-(prop-2-ynyl-oxy)but-2-enylthio]-*L*-homocysteine): 1.74–1.82(m, 1H), 1.93–1.99 (m, 1H), 2.54 (t, 1H,  $J = 7.6$  Hz), 3.15 (d, 2H,  $J = 5.8$  Hz), 3.20–3.33 (m, 1H), 3.45 (d, 1H,  $J = 2.4$  Hz), 3.98 (d, 2H,  $J = 4.3$  Hz), 4.12 (d, 2H,  $J = 2.4$  Hz), 5.64–5.67 (m, 2H), 7.54 (brs, 2H);  $^{13}C$  NMR (150 MHz,  $DMSO-d_6$ ):  $\delta$  26.62, 31.06, 32.04, 53.14, 56.53, 68.79, 77.27, 80.32, 128.38, 129.49, 169.15; MS(ESI)  $m/z$ : 244  $[M+H]^+$ ; HRMS: calculated for  $C_{11}H_{17}NO_3NaS$  ( $[M+Na]^+$ ) 266.0827, found 266.0822.

#### Protein expression and purification

Human MAT plasmids (full-length MATI and MATII) were a generous gift from Udo Oppermann (University of Oxford, [http://www.sgc.ox.ac.uk/structures/MAT1A\\_2obv.html](http://www.sgc.ox.ac.uk/structures/MAT1A_2obv.html) and [http://www.sgc.ox.ac.uk/structures/MM/MAT2AA\\_2p02\\_MM.html](http://www.sgc.ox.ac.uk/structures/MM/MAT2AA_2p02_MM.html)). To express the N-terminal 6  $\times$  His MATI and MATII, the plasmids were transformed into the *Escherichia coli* (DE3) Rosseta 2 strain and induced with 0.5 mM isopropyl  $\beta$ -D-1-thiogalactopyranoside (IPTG) at 17 °C for 16 h before harvesting. The resultant cell pellets were lysed with a buffer containing 50 mM Tris-HCl (pH 8.0), 50 mM NaCl, 5 mM  $\beta$ -mercaptoethanol, 25 mM imidazole, and the cocktail of Roche protease inhibitors and 5% (v/v) glycerol. The MATI and MATII proteins were then purified by Ni-NTA agarose resin (Qiagen) followed by a 5-ml HiTrap-Q Sepharose XL column (GE Healthcare). The fractions containing MATI and MATII proteins were combined and concentrated using an Amicon Ultra-10 K centrifugal filter device. The protein concentrations were determined with a Bradford assay kit (Bio-Rad) using bovine serum albumin (BSA) as a standard. The concentrated proteins were stored at  $-80$  °C before use. The MAT mutants were generated from the native plasmids with a Quik-Change site-directed mutagenesis kit (Agilent Technologies) with the vendor's protocols. The mutation sites of the plasmids were confirmed by DNA sequencing. All of the mutants were expressed and purified as described above for the native MATs.

#### Conventional HPLC analysis of SAM production by native MATs

A prior HPLC-based MAT activity assay was used to characterize the kinetics of native MATs [25]. This experiment was carried out as an established standard to evaluate the robustness of the newly developed LC-MS/MS-based assay in the current work. Briefly, the activities of native MATs were measured in 2 ml of reaction mixture containing 100 mM Tris-HCl (pH 8.0), 100 mM KCl, 2 mM  $MgCl_2$ , 8 mM glutathione, 2.5 mM ATP, 7.5  $\mu$ M MATs, and varied concentrations of methionine (up to 4 mM). The reaction mixture was incubated at ambient temperature (23 °C) with a 4-min interval within 20 min (a linear range of initial rates), and then a 300- $\mu$ l reaction aliquot was quenched with 300  $\mu$ l of 20%  $HClO_4$  aqueous solution. After centrifugation at 15,350g for 30 min, the supernatants containing SAM were resolved by reverse-phase HPLC using a DELTA PAK C18 column (15  $\mu$ m, 300  $\times$  3.9 mm) by monitoring at UV 260 nm. The triethylamine-acetic acid buffer (50 mM, pH 5.0) and methanol were premixed with the ratios of 98:2 (buffer A) and 50:50 (buffer B). SAM was eluted with buffer A for 30 min, followed by buffer B for 5 min, at a flow rate of 1 ml/min. The integrated peak areas at 260 nm were used to generate the standard curve with the known concentration of SAM and to quantify the SAM produced in the kinetic assay ( $\epsilon_{260} = 15,400$  L mol $^{-1}$  cm $^{-1}$  for SAM's adenine moiety).

#### LC-MS/MS-based MAT activity assay for heat map analysis

The reactions of MATs and their mutants were carried out in a reaction mixture containing 50 mM Tris-HCl (pH 8.0), 100 mM

KCl, 2 mM  $MgCl_2$ , 2.5 mM ATP, 7.5  $\mu$ M native or engineered MATs, and 2.5 mM methionine or SAAM in a final volume of 10  $\mu$ l. The active mutants were incubated with SAAM in a 96-well plate at ambient temperature (23 °C) for 8 to 10 h. The long incubation time, although saturating the signals of more reactive substrate-enzyme pairs, allowed maximizing the signals of less active substrate-enzyme pairs (96-well polymerase chain reaction [PCR] plates sealed with adhesive PRC sealing foil sheets should be used to avoid potential evaporation in particular for the latter step involved with heating). Subsequently, 1.0  $\mu$ l of 1.0 M citrate buffer was added into the reaction mixture, followed by incubation at 55 °C for 3.5 h, to convert the SAM/SAM analogues into the corresponding 5'-methylthioadenosine (MTA)/MTA analogues. This degradation procedure was previously reported to give a consistent yield of approximately 80% from SAM to MTA through intramolecular lactonization [30]. The reaction mixture was then diluted by a 1:100 ratio with double-distilled  $H_2O$  containing a known amount of SAH as the internal reference for MS analysis. Then 2  $\mu$ l of the diluted reaction mixture was injected into the 6410 tandem LC-MS/MS system for quantitative analysis. As a result, the dilution factor of "110" was applied here on calculating the concentrations of SAM/SAM analogues as described below.

The integrated peak areas for the MTA/MTA analogues and the SAH standards were quantified by the corresponding MRM modes using the 6410 tandem LC-MS/MS system. Prior to the MS analysis, the sample was applied to a Zorbax Eclipse XDB-C18 column (2.1  $\times$  50 mm, 3.5  $\mu$ m) for LC separation using a gradient elution system with buffer A (0.1%  $HCOOH$  in double-distilled  $H_2O$ ) and buffer B ( $CH_3CN$ ) of the following gradient: 0 to 0.5 min, 5 to 30% B; 0.5 to 5 min, 30% B; 5 to 7 min, 30 to 5% B. Integrated peak areas for all MTA/MTA analogues were compared with those of exogenously added SAH standards (see Fig. S1 in the online supplementary material as an example). Here SAM/SAM analogues in the enzymatic reactions were quantified on the basis of the relative peak ratios to the known amount of SAH rather than the absolute peak areas of MTA/MTA analogues (see below for details), a procedure that was implemented to avoid potential errors from the multiple-step operation.

Prior to quantification of the SAM/SAM analogues, a standard curve was generated by applying known concentrations of SAM/SAM analogues and equal concentrations of SAH (after the step of 1:100 dilution) under the conditions described above. The ratios of the peak areas between the SAH standard and the resultant MTA/MTA analogues were calculated to give the "correction factors" (see Fig. S1 as an example). The concentrations of SAM/SAM analogues in the chemoenzymatic reactions were then quantified from the converted MTA/MTA analogues according to the following equation:  $[SAM]_{\text{reaction}} = (\text{peak area of MTA/MTA analogues})/(\text{peak area of SAH}) \times [SAH]_{\text{standard}} \times \text{"correction factor"} \times \text{"dilution factor"}$ , where  $[SAM]_{\text{reaction}}$  is the concentration of SAM or SAM analogues generated in the enzymatic reaction, (peak area of MTA/MTA analogues)/(peak area of SAH) is the peak ratio obtained by the corresponding MRM MS,  $[SAH]_{\text{standard}}$  is the concentration of internal SAH standard added in the step of the 1:100 dilution, the "correction factor" was obtained as described from the standard curves generated with known concentrations of SAM and SAM analogues, and the "dilution factor" is "110" on counting the 1:10 dilution with 1.0 M citrate buffer and the subsequent 1:100 dilution with double-distilled  $H_2O$  as described above.

#### Characterization of kinetics of native and engineered MATs

To determine the apparent  $k_{\text{cat}}$  and  $K_m$  values of native MATI and MATII and their mutants with methionine or SAAMs as substrates, the assays were carried out as described above (the LC-MS/MS-based MAT assay) except that 100  $\mu$ l of reaction mixture

containing SAM or SAAMs (up to 4 mM) was used and linear initial velocities were measured within 20 min with a 4-min interval for native MATs with methionine as a substrate or within 60 min with a 10-min interval for engineered MATs with SAAMs as substrates. The steady-state kinetic parameters were obtained on fitting the initial velocities (the production of SAM or SAM analogues vs. the reaction time) against the concentrations of methionine or SAAMs with GraphPad Prism 5 software according to the standard Michaelis–Menten equation ( $v = k_{\text{cat}} \times [S]/(K_m + [S])$ ).

## Results and discussion

### Selection of SAAMs and engineered MATs

To systematically evaluate the substrate specificity of MAT variants, we prepared SAAMs **2** to **8** featured by their varied *S*-alkyl substituents (Scheme 1). The less sterically hindered *S*-ethyl analogue of methionine (SAAM **2**) was previously reported to be an active substrate of native MATs (yeast and rat), producing the corresponding *S*-ethyl analogue of SAM [31,32]. Using a similar synthetic method [28], SAAMs **3**, **4**, and **5** were obtained (see Materials and Methods and supplementary material). In addition, bulkier SAAMs **6**, **7**, and **8** were also synthesized given that the corresponding SAM analogues have been reported as SAM surrogates for multiple native or engineered methyltransferases [17,19–21]. Briefly, the treatment of methionine with benzyl chloride in concentrated HCl furnished *S*-benzyl-*L*-homocysteine [29]. Its benzyl moiety was then removed by sodium metal in liquid ammonia. The resultant sodium thiolate was readily reacted with the corresponding alkyl tosylates or bromides in dry ethanol to afford SAAMs **3** to **8** (see Materials and Methods). The general synthetic strategy for SAAMs **3** to **8** is featured by the use of the common precursor *S*-benzyl-*L*-homocysteine (Scheme 1). The collection of methionine derivatives contains characteristic *S*- $\beta$ -vinyl substituents (e.g., **3–8**) and terminal alkyne moiety (e.g., **6–8**). The former is essential for the efficient transalkylation from the corresponding SAM analogues, whereas the latter, after transalkylation to the targets, is amenable to copper-catalyzed azide–alkyne Huisgen cycloaddition (the click reaction) with azide-containing probes for further characterization of the labeled targets [9,17,21,23,33].

To identify and characterize potential MAT variants that can act on SAAMs **2** to **8**, we focused on the two isoforms of human MATs, MATI and MATII, whose primary sequences are conserved across species with liver-specific and ubiquitous localization (Fig. 3A), respectively [34]. On aligning the MAT sequences of different species, we can profile a cluster of conserved residues that account for binding the methyl moiety of the substrate methionine (I117, C120, V121, S247, and I322 for human MATI, PDB 2OBV; I117, G120, V121, S247, and I322 for human MATII, PDB 2P02) (Figs. 1 and 3A) [16]. To expand this region to accommodate bulky SAAMs for enzyme catalysis, we systematically replaced these residues with less sterically hindered hydrophobic amino acids individually (e.g., Ala, Gly) or in combination. Here a collection of 40 MAT mutants was expressed and purified for further characterization.

### Development of a sensitive, generally applicable LC–MS/MS-based activity assay for MATs with SAAMs as substrates

To measure the activity of native MATs, many prior approaches relied on HPLC to separate and quantify SAM via its characteristic UV absorbance at 260 nm ( $\epsilon_{260} = 15,400 \text{ L mol}^{-1} \text{ cm}^{-1}$  for SAM's adenine moiety) [25]. However, given the inherent instability of SAM (and of many SAM analogues as well) and the low sensitivity of UV detection [18,19], we envisioned a more robust assay (Fig. 2)

through the quantitative conversion of the reaction product SAM (or SAM analogues) to MTA (or the corresponding *S*-alkylthioadenosines for SAM analogues) (55 °C in citrate buffer for 3.5 h as implemented before for MTA synthesis; see Materials and Methods and supplementary material) [30]. After the acidic degradation in a 96-well format, followed by centrifugation and adding SAH as an internal standard, the reaction mixture was then analyzed by HPLC–MS/MS. The amount of SAM (5  $\mu\text{M}$ –1 mM in a 10- $\mu\text{l}$  reaction mixture) is linearly converted to MTA as quantified by HPLC–MS/MS (data not shown). The LC–MS/MS-based assay was further validated on comparing its kinetic data with those generated by the conventional HPLC-based MAT assay (see results below).

The newly developed LC–MS/MS-based activity assay for MATs is highly sensitive and generally applicable. Under the current assay setting, we were able to process a 2% aliquant of a 10- $\mu\text{l}$  reaction sample (after 1:100 dilution) for the MS analysis and detected as little as 0.1 pmol of MTA (equivalent to 2% aliquant of 5  $\mu\text{M}$  SAM in a 10- $\mu\text{l}$  reaction mixture as described above). Such sensitivity is 3 orders of magnitude higher than that of the conventional HPLC-coupled UV spectroscopy method, which typically requires a 300- $\mu\text{l}$  reaction mixture for each time point [21,25]. The LC–MS/MS-based assay format is convenient in comparison with the conventional MAT assay using radioactive ATP or methionine [26], which is sensitive but must deal with expensive and less environmentally friendly materials. Our LC–MS/MS-based MAT activity is also generally applicable to engineered MATs with diverse SAAMs as substrates because the daughter ions of the corresponding *S*-alkylthioadenosines can be readily selected with the readily altered MS/MS detection mode (see Materials and Methods above and the results below). In addition, our LC–MS/MS-based MAT activity assay was designed in a mix-then-measure format and to handle a small volume of reaction samples (10  $\mu\text{l}$  in the current format), which can be further improved and adapted by automatic liquid dispensers into a high-throughput format. In terms of sensitivity and general application, our MAT activity assay is comparable to a newly reported spectroscopic MAT assay, which quantifies the enzyme-coupled production of NADPH from the reaction byproduct pyrophosphate [27]. However, the latter assay is not tolerant to the presence of interfering metabolites (e.g., pyrophosphate, glucose 6-phosphate) and, thus, is not suitable for evaluating native or engineered MATs in complex cellular settings. In contrast, the LC–MS/MS-based MAT activity can be implemented to examine native or engineered MATs under cellular settings by selectively monitoring the ions of interest (see Materials and Methods). Admittedly, the current LC–MS/MS MAT assay requires access to a specialized LC–MS/MS instrument, which might not be generally available. It remains to be determined whether the current assay format can be adapted for other HPLC–MS instruments.

### Identification of MAT variants recognizing SAAMs as substrates

After validating the MS-based activity MAT assay, we applied it to screen the MAT mutants against SAAMs **2** to **8** in the presence of a physiologically relevant concentration of ATP (2.5 mM) [35]. As displayed in the heat map, the I117A variants of both MATI and MATII demonstrated broad substrate specificity and high efficiency in processing the SAAMs as substrates (Fig. 3B and C). Among the examined mutant–substrate pairs, most of the MAT mutants showed detectable activity with the less sterically hindered *S*-ethyl analogue of methionine **2** as a substrate (Fig. 3B and C). Such wide substrate specificity dropped dramatically from SAAM **3** to SAAM **5**. In particular, many MAT mutants displayed barely detectable ability to process bulkier methionine analogues such as SAAMs **6**, **7**, and **8**. However, among the MAT mutants, the two I117A variants still showed relatively higher efficiency to act on all of the examined SAAMs (Fig. 3B and C). Given that the native MATs show

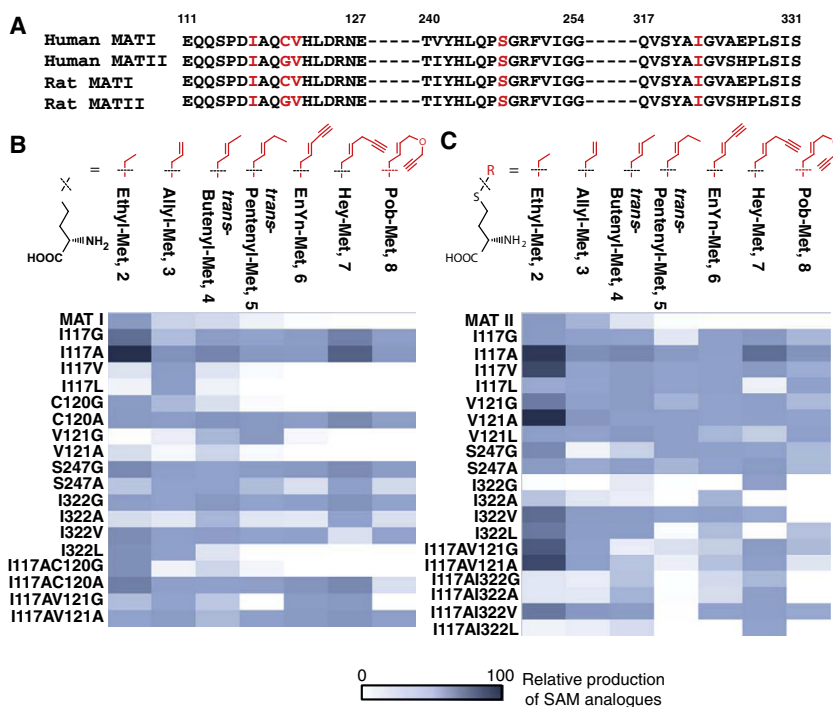


**Fig. 3.** Sequence alignment of MATs and reactivity heat map of MATI and MATII variants against SAAMs as substrates. (A) Sequence alignment of human and rat MATs. Highlighted are the conserved residues (I117, C120, V121, S247, and I322 of human MATs), which account for binding the methyl moiety of the substrate methionine on the basis of the structures of human MATI and MATII (PDB 2OBV and 2P02). (B,C) Native and MATI and MATII mutants were screened against SAAMs **2** to **8** in a combinatorial manner. The results for MATI variants (B) and MATII variants (C) are presented in a heat map format. The amount of the produced SAM analogues was normalized to that of the ethyl-SAM produced by the corresponding I117A mutants.

barely detectable activity toward SAAMs **6** to **8** (Fig. 3B and C), mutating I117 is essential for MATs to gain the ability to recognize these bulky SAAMs.

#### Kinetic analysis of native and I117A MATs

Because the I117A mutants of MATI and MATII are most effective in processing SAAMs **2** to **8**, we implemented the above-established LC-MS/MS MAT activity assay to characterize their kinetics (Fig. 4, S8, and Table 1, S1). Apparent kinetic parameters obtained for native MATI, MATII, and methionine using the newly developed assay are consistent with those obtained using the conventional HPLC-based MAT assay except that a much greater amount of materials needed to be used in the latter assay [25]. Thus, this consistency validated the robustness of the current LC-MS/MS-based MAT assay for the current application (Fig. 4, S8, and Table 1, S1). Consistent with the heat map comparison (Fig. 3B and C), the catalytic turnover ( $k_{\text{cat}}$  values) of native MATI and MATII dropped approximately 50-fold with SAAM **2** and was barely measurable for the bulkier SAAMs **3** to **8**. Although  $k_{\text{cat}}$  values of the I117A variants of MATI and MATII are 5-fold lower than those of native MATI and MATII toward methionine, the I117A mutants showed comparable  $k_{\text{cat}}$  values between methionine and SAAM **2** (<2-fold decrease of its  $k_{\text{cat}}$  value). The broad substrate specificity of the MAT I117A variants is further maintained for the bulkier SAAMs **3** to **5** and SAAM **7** (3- to 7-fold difference in their  $k_{\text{cat}}$  values from **2**). For the I117A variants, SAAMs **6** and **8**, which contain the sterically rigid alkynyl-*trans*-vinyl moiety and the bulkiest propargyl-oxy-*trans*-butenyl moiety, respectively, are the least reactive substrates, as shown by their 30- to 100-fold decrease of  $k_{\text{cat}}$  values, in contrast to methionine **1** and SAAM **2**.

Despite up to 100-fold variation of the  $k_{\text{cat}}$  values of native MATI and MATII and their I117A variants with methionine and SAAM as substrates, the corresponding  $K_{\text{m}}$  values are within the 2- to 3-fold

difference for the same set of SAAMs. On comparing the overall catalysis efficiency ( $k_{\text{cat}}/K_{\text{m}}$  values), methionine **1** and most SAAMs

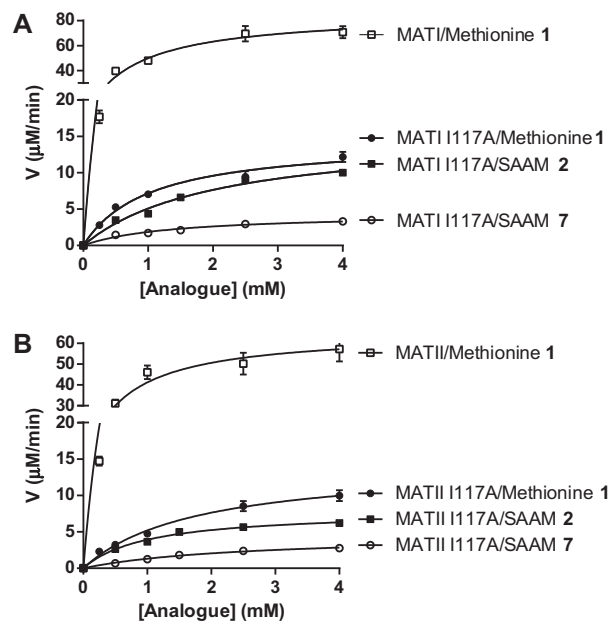


**Fig. 4.** Representative Michaelis–Menten kinetics of methionine analogues paired with MATI variants (A) and MATII variants (B). Here  $k_{\text{cat}} = 11.5 \text{ min}^{-1}$  and  $K_{\text{m}} = 0.73 \text{ mM}$  for native MATI with methionine **1** as substrate;  $k_{\text{cat}} = 1.9 \pm 0.1$ ,  $2.1 \pm 0.2$ , and  $0.59 \pm 0.6 \text{ min}^{-1}$  and  $K_{\text{m}} = 1.0 \pm 0.2$ ,  $2.0 \pm 0.5$ , and  $1.4 \pm 0.4 \text{ mM}$  for MATI I117A with methionine **1**, SAAM **2**, and SAAM **7** as substrates, respectively;  $k_{\text{cat}} = 8.8 \pm 0.6 \text{ min}^{-1}$  and  $K_{\text{m}} = 0.6 \pm 0.1 \text{ mM}$  for native MATII with methionine **1** as substrate;  $k_{\text{cat}} = 1.9 \pm 0.1$ ,  $1.1 \pm 0.1$ , and  $0.62 \pm 0.05 \text{ min}^{-1}$  and  $K_{\text{m}} = 1.8 \pm 0.3$ ,  $1.0 \pm 0.4$ , and  $2.5 \pm 0.4 \text{ mM}$  for MATII I117A with methionine **1**, SAAM **2**, and SAAM **7** as substrates, respectively. See Fig. S8 in the supplementary material for the complete set of kinetic data.

**Table 1**  
Relative  $k_{\text{cat}}$  and  $K_{\text{m}}$  values of native MATI and MATII and their I117A variants with methionine **1** or SAAMs **2** to **8**



SAAM:	1	2	3	4	5	6	7	8
Native MATI	$k_{\text{cat}} = 1.0$ $K_{\text{m}} = 1.0$ $k_{\text{cat}}/K_{\text{m}} = 1.0$	$k_{\text{cat}} = 0.017$ $K_{\text{m}} = 2.3$ $k_{\text{cat}}/K_{\text{m}} = 0.0070$	ND	ND	ND	ND	ND	ND
MATI I117A	$k_{\text{cat}} = 0.17$ $K_{\text{m}} = 1.4$ $k_{\text{cat}}/K_{\text{m}} = 0.12$	$k_{\text{cat}} = 0.18$ $K_{\text{m}} = 2.8$ $k_{\text{cat}}/K_{\text{m}} = 0.064$	$k_{\text{cat}} = 0.052$ $K_{\text{m}} = 1.2$ $k_{\text{cat}}/K_{\text{m}} = 0.042$	$k_{\text{cat}} = 0.060$ $K_{\text{m}} = 0.58$ $k_{\text{cat}}/K_{\text{m}} = 0.11$	$k_{\text{cat}} = 0.024$ $K_{\text{m}} = 1.0$ $k_{\text{cat}}/K_{\text{m}} = 0.024$	$k_{\text{cat}} = 0.010$ $K_{\text{m}} = 0.81$ $k_{\text{cat}}/K_{\text{m}} = 0.013$	$k_{\text{cat}} = 0.051$ $K_{\text{m}} = 1.9$ $k_{\text{cat}}/K_{\text{m}} = 0.027$	$k_{\text{cat}} = 0.0065$ $K_{\text{m}} = 5.1$ $k_{\text{cat}}/K_{\text{m}} = 0.0013$
Native MATII	$k_{\text{cat}} = 1.0$ $K_{\text{m}} = 1.0$ $k_{\text{cat}}/K_{\text{m}} = 1.0$	$k_{\text{cat}} = 0.015$ $K_{\text{m}} = 1.7$ $k_{\text{cat}}/K_{\text{m}} = 0.0081$	ND	ND	ND	ND	ND	ND
MATII I117A	$k_{\text{cat}} = 0.22$ $K_{\text{m}} = 3.0$ $k_{\text{cat}}/K_{\text{m}} = 0.074$	$k_{\text{cat}} = 0.12$ $K_{\text{m}} = 1.7$ $k_{\text{cat}}/K_{\text{m}} = 0.070$	$k_{\text{cat}} = 0.034$ $K_{\text{m}} = 0.80$ $k_{\text{cat}}/K_{\text{m}} = 0.042$	$k_{\text{cat}} = 0.062$ $K_{\text{m}} = 8.5$ $k_{\text{cat}}/K_{\text{m}} = 0.0074$	$k_{\text{cat}} = 0.033$ $K_{\text{m}} = 5.3$ $k_{\text{cat}}/K_{\text{m}} = 0.0063$	$k_{\text{cat}} = 0.0025$ $K_{\text{m}} = 10$ $k_{\text{cat}}/K_{\text{m}} = 0.00025$	$k_{\text{cat}} = 0.071$ $K_{\text{m}} = 4.3$ $k_{\text{cat}}/K_{\text{m}} = 0.016$	$k_{\text{cat}} = 0.011$ $K_{\text{m}} = 4.5$ $k_{\text{cat}}/K_{\text{m}} = 0.0024$

Note. Apparent kinetic parameters ( $k_{\text{cat}}$  and  $K_{\text{m}}$  values) were obtained in the presence of 2.5 mM ATP and varied concentrations of SAAMs as substrates. The relative kinetic parameters were obtained by dividing their  $k_{\text{cat}}$  and  $K_{\text{m}}$  values by those of the I117A variants. Here  $k_{\text{cat}} = 11.5 \pm 0.7 \text{ min}^{-1}$  and  $K_{\text{m}} = 0.7 \pm 0.1 \text{ mM}$  for native MATI and methionine;  $k_{\text{cat}} = 8.8 \pm 0.6 \text{ min}^{-1}$  and  $K_{\text{m}} = 0.6 \pm 0.1 \text{ mM}$  for native MATII and methionine. The kinetic parameters of native MATs with methionine were validated by the conventional HPLC assay (see Fig. S9 in supplementary material). See Fig. 4 for Michaelis–Menten curves of the representative SAAM–mutant pairs. ND, not detectable. See Table S1 for the complete set of kinetic data with error bars.

(**2–7** but not **8**) are suitable substrates of the I117A variant of MATI (with 10-fold difference of the  $k_{\text{cat}}/K_{\text{m}}$  values for **2–7**). In contrast, the  $k_{\text{cat}}/K_{\text{m}}$  values of the I117A variant of MATII is more substrate dependent with the higher preference for SAAMs **1** to **4** and SAAM **7** than for SAAMs **5**, **6**, and **8** (<5-fold vs. 30- to 100-fold drop of their  $k_{\text{cat}}/K_{\text{m}}$  values). Among the SAAMs containing terminal-alkyne amenable to the click reaction (**6–8**), SAAM **7** is the most reactive substrate for both MATI and MATII I117A variants, with a slight preference for the former (<2-fold difference of the  $k_{\text{cat}}/K_{\text{m}}$  values between the two variants; 2- to 100-fold difference of the  $k_{\text{cat}}/K_{\text{m}}$  values between SAAM **7** and SAAM **6** or **8**).

#### Relevant steady-state parameters of engineered MATs with bulky SAAMs as substrates

The methionine binding pocket of native human MATI and MATII appears not to be spacious enough to accommodate bulky SAAMs, as reflected by the significant decrease or complete loss of enzymatic activities toward the bulky SAAMs **2** to **8**. In contrast, removal of several bulky amino acids (e.g., I117, C120, V121, S247, and I332 in Fig. 3) adjacent to the S-methyl binding site of the substrate methionine readily expands the binding pocket to accommodate these bulky SAAMs (Fig. 3). The slight variation of  $K_{\text{m}}$  values (<10-fold) of the most active MATI and MATII I117A mutants for the SAAMs ( $K_{\text{m}}$  values in Table 1) further argues that these MATI and MATII variants gain comparable affinity to the structurally diverse SAAMs as substrates. This result is remarkable given the small decrease of size from Ile to Ala versus the significant increase of size from methionine to SAAM **8**. Here we also noticed that the heat maps for SAAMs agree well between native MATI and MATII, their I117A mutants, but not their I117V mutants (Fig. 3B). The striking gain-of-function activities of certain MATI and MATII mutants toward SAAMs and the difference for others (e.g., I117V) could be attributed to specific conformational changes associated with each variant. However, more structural characterization is required to provide a molecular-level rationale about how a single point mutation can lead to such difference among the closely related MAT variants.

Our data further suggest that the binding of SAAMs **2** to **8**, although necessary, is insufficient for the MATI and MATII I117A

mutants to act on these compounds as substrates. In contrast to the less than 10-fold variation of  $K_{\text{m}}$  values, which reflects the enzyme–substrate binding along the reaction path, the more than 100-fold fluctuation of  $k_{\text{cat}}$  values (Fig. 4 and Table 1) plays a more significant role in the overall enzyme catalysis. The MAT-catalyzed adenylation on methionine is expected to go through a linear  $S_{\text{N}}2$  transition state with methionine and pyrophosphate as the nucleophile and leaving group, respectively (Figs. 1 and 5) [36]. Given that a  $k_{\text{cat}}$  value likely reflects the enzymatic efficiency at this chemical step, the activities of the MATI and MATII I117A mutants on the SAAMs can be ranked as **2** > **3**, **4**, **5**, **7** > **6**, **8** according to their respective  $k_{\text{cat}}$  values. Such a trend features the SAAMs containing smaller S-alkyl substituents as the more active substrates (e.g., **2**, **7**) versus those containing bulky or rigid S-alkyl substituents as more inert substrates (e.g., **6**, **8**). We argued that this difference likely arises from the ability of the former to maintain the linear  $S_{\text{N}}2$  transition state of native MATI and MATII, as reflected by the higher  $k_{\text{cat}}$  value at the chemical step (Fig. 5). In contrast, the bulkiness or rigidity may restrict the latter from forming an optimized linear  $S_{\text{N}}2$  transition state along the reaction path (Fig. 5).

#### Most active MAT variants with matched SAAMs as substrates

On comparing  $k_{\text{cat}}$ ,  $K_{\text{m}}$ , and  $k_{\text{cat}}/K_{\text{m}}$  values for the panel of substrates (methionine or SAAMs), we concluded that the MATI and MATII I117A mutants have the highest activities toward methionine (Table 1). Here SAAM **7** is only 4-fold less reactive than methionine as the substrate of the MATI and MATII I117A mutants. This result is consistent with the prior observation that SAAM **7** can be processed by the MATII I117A mutant to produce the corresponding SAM analogue within living cells [16]. The prior work also showed that SAAM **7** is a better substrate of the MATII variant than is SAAM **8** [16]. Such a finding is readily reflected by the 7-fold higher  $k_{\text{cat}}$  (or  $k_{\text{cat}}/K_{\text{m}}$ ) value of SAAM **7** in comparison with SAAM **8**. The intracellular concentration of methionine varies from 150 to 280 pmol/ $10^7$  cells [37]. In previous work, we showed that the incubation of 1 mM SAAM **7** in combination with methionine depletion in the growth medium is sufficient for the MATII I117A variant to produce the corresponding SAM analogue with its intracellular concentration comparable to that of SAM in a native setting [16].

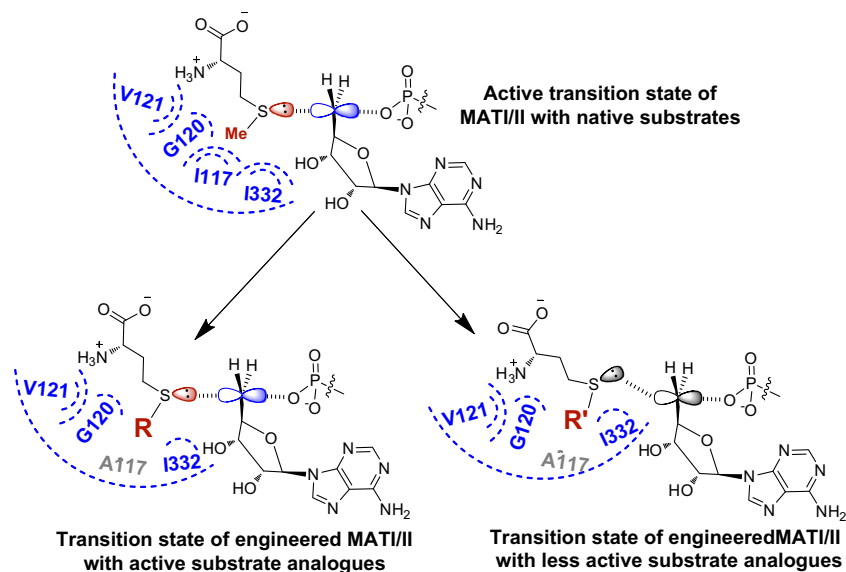


**Fig. 5.** Expected transition state structures of MAT-catalyzed adenylation. Top panel: Proposed linear  $S_N2$  transition state of the native enzyme with methionine and ATP as substrates; Bottom panel: Expected transition states of engineered MATs with methionine analogues and ATP as substrates. The active transition state (left) is featured by its linear  $S_N2$  configuration, in contrast to the less active enzyme–substrate intermediate (right).

The comparable  $k_{cat}$ ,  $K_m$ , and  $k_{cat}/K_m$  values between SAAMs and methionine (4-fold difference for SAAM 7) for the MATI and MATII I117A variants (Table 1) suggest that complete depletion of methionine might not be necessary for in-cell production of the corresponding SAM analogues.

## Conclusion

Here we have described a sensitive HPLC–MS/MS-based MAT assay to characterize native and engineered MATs with methionine and SAAMs as substrates. In contrast to the several conventional MAT activity assays, which are of low sensitivity and have limited application, our assay is characterized by its high sensitivity and general applicability. With the aid of this robust assay, more than 40 MATI and MATII mutants were screened against SAM and 7 SAAMs. Here MATI I117A was identified to be the most active MATI variant by acting on structurally diverse SAAMs. The relatively constant  $K_m$  values versus largely altered  $k_{cat}$  values of MATI I117A across SAAMs 2 to 8 further argue that, although the MAT variant is able to bind bulky SAAMs with comparable affinity as native MATI and MATII bind methionine, such binding is not sufficient to promote enzymatic catalysis. The most reactive substrates, such as 3 and 7 for the MATI and MATII I117A variants, may be featured by their ready formation of the active  $S_N2$  transition state. In contrast, the less reactive substrates, such as 6 and 8, cannot be processed because of the potential disruption of the enzyme transition states by their structurally rigid or sterically hindered S-alkyl substituents. These results collectively argue that the flexibility and size of S-alkyl substituents are important parameters for SAAMs to be recognized as substrates by the engineered MATs. More important, the current work enabled us to identify the I117A variant of MATI as a more general MAT variant to process SAAMs into corresponding SAM analogues.

As the primary biological methyl donor, SAM plays a pivotal role under a variety of physiological settings. For instance, protein methyltransferases, which transfer the methyl group from SAM to the specific Lys or Arg residues of substrates, are essential for epigenetic regulation [12,13]. Given the potential utility of the terminal-alkyne-containing SAM analogues to label substrates of

methyltransferases [12,13,16–18], the revealed structure–activity relationship of MAT variants and SAAMs can provide further guidance to couple two sets of enzymes for more efficient substrate labeling inside living cells. The high sensitivity and robustness of the current MS-based MAT assay also permits the analysis of the corresponding metabolites in cell lysates.

## Acknowledgments

We thank Kabirul Islam for providing several SAAMs, Udo Oppermann for providing MAT plasmids, and Tony Taldone for developing the HPLC–MS/MS method. We thank Ian Bothwell for comments on the manuscript. We are grateful for the financial support from the National Institute of General Medical Sciences (1R01GM096056), the National Institute of Health (NIH) Director's New Innovator Award Program (1DP2-OD007335), the March of Dimes Foundation (Basil O'Connor Starter Scholar Award), the Starr Cancer Consortium, and the Alfred W. Bressler Scholars Endowment Fund.

## Appendix A. Supplementary data

Supplementary data associated with this article can be found, in the online version, at <http://dx.doi.org/10.1016/j.ab.2013.12.026>.

## References

- [1] S. Klimasauskas, E. Weinhold, A new tool for biotechnology: AdoMet-dependent methyltransferases, *Trends Biotechnol.* 25 (2007) 99–104.
- [2] S.C. Lu, S-Adenosylmethionine, *Int. J. Biochem. Cell Biol.* 32 (2000) 391–395.
- [3] J. Kim, H. Xiao, J.B. Bonanno, C. Kalyanaraman, S. Brown, X. Tang, N.F. Al-Obaidi, Y. Patskovsky, P.C. Babbitt, M.P. Jacobson, Y.S. Lee, S.C. Almo, Structure-guided discovery of the metabolite carboxy-SAM that modulates tRNA function, *Nature* 498 (2013) 123–126.
- [4] B.J. Landgraf, S.J. Booker, Biochemistry: the ylide has landed, *Nature* 498 (2013) 45–47.
- [5] F. Yan, J.M. LaMarre, R. Röhrich, J. Wiesner, H. Jomaa, A.S. Mankin, D.G. Fujimori, RimN and Cfr are radical SAM enzymes involved in methylation of ribosomal RNA, *J. Am. Chem. Soc.* 132 (2010) 3953–3964.
- [6] Y. Zhang, X. Zhu, A.T. Torelli, M. Lee, B. Dzikovski, R.M. Koralewski, E. Wang, J. Freed, C. Krebs, S.E. Ealick, H. Lin, Diphthamide biosynthesis requires an organic radical generated by an iron–sulphur enzyme, *Nature* 465 (2010) 891–896.

- [7] A.W. Struck, M.L. Thompson, L.S. Wong, J. Micklefield, S-Adenosyl-L-methionine-dependent methyltransferases: highly versatile enzymes in biocatalysis, biosynthesis, and other biotechnological applications, *ChemBioChem* 13 (2012) 2642–2655.
- [8] Q. Lin, F. Jiang, P.G. Schultz, N.S. Gray, Design of allele-specific protein methyltransferase inhibitors, *J. Am. Chem. Soc.* 123 (2001) 11608–11613.
- [9] W. Peters, S. Willnow, M. Duisken, H. Kleine, T. Macherey, K.E. Duncan, D.W. Litchfield, B. Lüscher, E. Weinhold, Enzymatic site-specific functionalization of protein methyltransferase substrates with alkynes for click labeling, *Angew. Chem. Int. Ed.* 49 (2010) 5170–5173.
- [10] J. Li, H. Wei, M.M. Zhou, Structure-guided design of a methyl donor cofactor that controls a viral histone H3 lysine 27 methyltransferase activity, *J. Med. Chem.* 54 (2011) 7734–7738.
- [11] D.F. Iwig, A.T. Grippe, T.A. McIntyre, S.J. Booker, Isotope and elemental effects indicate a rate-limiting methyl transfer as the initial step in the reaction catalyzed by *Escherichia coli* cyclopropane fatty acid synthase, *Biochemistry* 43 (2004) 13510–13524.
- [12] R. Wang, M. Luo, A journey toward bioorthogonal profiling of protein methylation inside living cells, *Curr. Opin. Chem. Biol.* 17 (2013) 729–731.
- [13] M. Luo, Current chemical biology approaches to interrogate protein methyltransferases, *ACS Chem. Biol.* 7 (2012) 443–463.
- [14] J.M. Winter, G. Chiou, I.R. Bothwell, W. Xu, N.K. Garg, M. Luo, Y. Tang, Expanding the structural diversity of polyketides by exploring the cofactor tolerance of an inline methyltransferase domain, *Org. Lett.* 15 (2013) 3774–3777.
- [15] K. Islam, Y. Chen, H. Wu, I.R. Bothwell, G.J. Blum, H. Zeng, A. Dong, W. Zheng, J. Min, H. Deng, M. Luo, Defining efficient enzyme-cofactor pairs for bioorthogonal profiling of protein methylation, *Proc. Natl. Acad. Sci. USA* 110 (2013) 16778–16783.
- [16] R. Wang, K. Islam, Y. Liu, W. Zheng, H. Tang, N. Lailler, G. Blum, H. Deng, M. Luo, Profiling genome-wide chromatin methylation with engineered posttranslational apparatus within living cells, *J. Am. Chem. Soc.* 135 (2013) 1048–1056.
- [17] K. Islam, I. Bothwell, Y. Chen, C. Sengelaub, R. Wang, H. Deng, M. Luo, Bioorthogonal profiling of protein methylation using azido derivative of S-adenosyl-L-methionine, *J. Am. Chem. Soc.* 134 (2012) 5909–5915.
- [18] I.R. Bothwell, K. Islam, Y. Chen, W. Zheng, G. Blum, H. Deng, M. Luo, S-adenosyl-L-selenomethionine cofactor analogue as a reporter of protein methylation, *J. Am. Chem. Soc.* 134 (2012) 14905–14912.
- [19] K. Islam, W. Zheng, H. Yu, H. Deng, M. Luo, Expanding cofactor repertoire of protein lysine methyltransferase for substrate labeling, *ACS Chem. Biol.* 6 (2011) 679–684.
- [20] R. Wang, G. Ibáñez, K. Islam, W. Zheng, G. Blum, C. Sengelaub, M. Luo, Formulating a fluorogenic assay to evaluate S-adenosyl-L-methionine analogues as protein methyltransferase cofactors, *Mol. Biosyst.* 7 (2011) 2970–2981.
- [21] R. Wang, W. Zheng, H. Yu, H. Deng, M. Luo, Labeling substrates of protein arginine methyltransferase with engineered enzymes and matched S-adenosyl-L-methionine analogues, *J. Am. Chem. Soc.* 133 (2011) 7648–7651.
- [22] J.M. Lipson, M. Thomsen, B.S. Moore, R.P. Clausen, J.J. La Clair, M.D. Burkart, A tandem chemoenzymatic methylation by S-adenosyl-L-methionine, *ChemBioChem* 14 (2013) 950–953.
- [23] C. Dalhoff, G. Lukinavicius, S. Klimasauskas, E. Weinhold, Direct transfer of extended groups from synthetic cofactors by DNA methyltransferases, *Nat. Chem. Biol.* 2 (2006) 31–32.
- [24] G. Cantoni, The nature of the active methyl donor formed enzymatically from L-methionine and adenosinephosphate, *J. Am. Chem. Soc.* 74 (1952) 2942–2943.
- [25] V. Kamarthapu, K.V. Rao, P.N. Srinivas, G.B. Reddy, V.D. Reddy, Structural and kinetic properties of *Bacillus subtilis* S-adenosylmethionine synthetase expressed in *Escherichia coli*, *Biochim. Biophys. Acta* 1784 (2008) 1949–1958.
- [26] G.D. Markham, E.W. Hafner, C.W. Tabor, H. Tabor, S-Adenosylmethionine synthetase from *Escherichia coli*, *J. Biol. Chem.* 255 (1980) 9082–9092.
- [27] S.P. Zano, P. Bhansali, A. Luniwal, R.E. Viola, Alternative substrates selective for S-adenosylmethionine synthetases from pathogenic bacteria, *Arch. Biochem. Biophys.* 536 (2013) 64–71.
- [28] J. Jiracek, M. Collinsova, I. Rosenberg, M. Budesinsky, E. Protivinska, H. Netusilova, T.A. Garrow, S-Alkylated homocysteine derivatives: new inhibitors of human betaine-homocysteine S-methyltransferase, *J. Med. Chem.* 49 (2006) 3982–3989.
- [29] B. Peric Simov, F. Wuggenig, K. Mereiter, H. Andres, J. France, P. Schnell, F. Hammerschmidt, Direct chemical synthesis of chiral methanol of 98% ee and its conversion to [<sup>2</sup>H<sub>1</sub>,<sup>3</sup>H]methyl tosylate and [<sup>2</sup>H<sub>1</sub>,<sup>3</sup>H-methyl]methionine, *J. Am. Chem. Soc.* 127 (2005) 13934–13940.
- [30] J.A. Gutierrez, M. Luo, V. Singh, L. Li, R.L. Brown, G.E. Norris, G.B. Evans, R.H. Furneaux, P.C. Tyler, G.F. Painter, D.H. Lenz, V.L. Schramm, Picomolar inhibitors as transition-state probes of 5'-methylthioadenosine nucleosidases, *ACS Chem. Biol.* 2 (2007) 725–734.
- [31] J.H. Alix, Molecular aspects of the in vivo and in vitro effects of ethionine, an analog of methionine, *Microbiol. Rev.* 46 (1982) 281–295.
- [32] W.R. Leopold, J.A. Miller, E.C. Miller, Comparison of some carcinogenic, mutagenic, and biochemical properties of S-vinylhomocysteine and ethionine, *Cancer Res.* 42 (1982) 4364–4374.
- [33] G. Blum, I.R. Bothwell, K. Islam, M. Luo, Profiling protein methylation with cofactor analog containing terminal alkyne functionality, *Curr. Protoc. Chem. Biol.* 5 (2013) 67–88.
- [34] J.M. Mato, L. Alvarez, P. Ortiz, M.A. Pajares, S-Adenosylmethionine synthesis: molecular mechanisms and clinical implications, *Pharmacol. Ther.* 73 (1997) 265–280.
- [35] F.M. Gribble, G. Loussouarn, S.J. Tucker, C. Zhao, C.G. Nichols, F.M. Ashcroft, A novel method for measurement of submembrane ATP concentration, *J. Biol. Chem.* 275 (2000) 30046–30049.
- [36] G.D. Markham, F. Takusagawa, A.M. Dijulio, C.W. Bock, An investigation of the catalytic mechanism of S-adenosylmethionine synthetase by QM/MM calculations, *Arch. Biochem. Biophys.* 492 (2009) 82–92.
- [37] R. Carmel, D.W. Jacobsen (Eds.), *Homocysteine in Health and Disease*, Cambridge University Press, Cambridge, UK, 2001.